The Journal of Veterinary Medical Science

NOTE

Surgery

A case of hydronephrosis due to intrarenal ureteral obstruction in a Japanese Black calf

Reiichiro SATO[1,2)]*, Takuya HIRAI[1,2)], Asmaa A. HEGAZY[1)], Mutsumi NAKAI[2)], Yukiko SATO[3)], Kazutaka YAMADA[4)], Hiroyuki SATOH[1,2)], Adrian STEINER[5)]

[1)]Graduate School of Medicine and Veterinary Medicine, University of Miyazaki, Miyazaki, Japan
[2)]Faculty of Agriculture, University of Miyazaki, Miyazaki, Japan
[3)]Miyazaki Agricultural Mutual Aid Association, Miyazaki, Japan
[4)]School of Veterinary Medicine, Azabu University, Kanagawa, Japan
[5)]Vetsuisse Faculty, Clinic for Ruminants, University of Bern, Bern, Switzerland

J Vet Med Sci
86(11): 1162–1167, 2024
doi: 10.1292/jvms.24-0173

Received: 2 May 2024
Accepted: 19 September 2024
Advanced Epub:
27 September 2024

ABSTRACT. A 23-day-old Japanese Black female calf presented with distension of the lower abdomen. Abdominal ultrasonography revealed a cystic structure with fluid accumulation and moderate echoluminance in the right abdominal cavity. Ultrasonography and contrast-enhanced computed tomography revealed congenital hydronephrosis due to narrowing of the intrarenal ureter, and right kidney resection was performed. Blood urea nitrogen and serum creatinine levels, which were within reference values preoperatively, peaked on the third postoperative day and gradually decreased afterward until reaching preoperative values on the tenth day. In bovine hydronephrosis, nephrectomy may provide a favorable prognosis if one kidney is intact. Moreover, this case suggests that blood tests immediately after surgery are not suitable for evaluating residual kidneys.

KEYWORDS: calf, computed tomography, hydronephrosis, nephrectomy, ultrasonography

Renal disease in cattle is generally diagnosed based on clinical signs, and blood test, urinalysis, rectal examination, cystoscopy, and ultrasonography findings [10, 11]. Elevated blood urea nitrogen (BUN) and serum creatinine (Cre) levels may indicate renal dysfunction [17, 28]. Rectal palpation of intra-abdominal organs is of great diagnostic value but is not possible in calves or juveniles. Ultrasonography of the kidneys is useful for noninvasive determination of the nature of renal masses, including differentiating cystic from solid masses [16] and liquid from blood-filled masses [8], as well as evaluating the shape and size of intraperitoneal masses and organs [7].

Hydronephrosis is a condition in which the urinary tract distal to the renal pelvis is obstructed or narrowed, while the renal pelvis and renal cups are dilated [5, 18, 23]. Hydronephrosis in humans is caused by congenital diseases [19], stones [4, 14, 22], and chronic infections [3], with congenital causes being the most common in children [13]. In cattle, there have been reports of infection in adult cattle [12] and urinary tract obstruction due to urinary stones [1] or polyps [26] in the urethra; however, there have been no such reports in calves less than one month old.

For the treatment of human hydronephrosis, surgical intervention is generally reserved for cases with signs of obstructive damage, and the type of surgery is determined according to the anatomical and functional status of the renal unit [6, 15, 24].

This paper describes the diagnosis, treatment, and prognosis of hydronephrosis in a calf, caused by congenital obstruction of the intrarenal ureter, and the results of the hemodynamics and biochemical tests after nephrectomy.

A female Japanese Black calf presented with mild distension of the lower abdomen at the age of 23 days. Ultrasonography performed by the referral veterinarian revealed a large mass with fluid retention in the right abdominal cavity, extending from the right lower flank to the liver. Over the following few days, the mass gradually increased in size; therefore, the calf was referred to the Miyazaki University Veterinary Teaching Hospital for advanced examination, diagnosis, and treatment.

On admission, the calf aged 36 days and weighed 42 kg. The calf's heart rate, respiratory rate, and rectal temperature were 104 beats/min, 40 breaths/min, and 39.1°C, respectively. Although respiration was a little rapid, the general condition was good. The right and left lower abdomen were distended with a pear-shaped appearance, and a mass in the right abdominal cavity was identified by bimanual extra abdominal palpation.

The complete blood test results were within normal limits, with a white blood cell count of 6,600 cells/μL, red blood cell count of 973

*Correspondence to: Sato R: r-sato@cc.miyazaki-u.ac.jp, Graduate School of Medicine and Veterinary Medicine, University of Miyazaki, 1-1 Gakuen Kibanadai-nishi, Miyazaki 889-2192, Japan

× 10^4 cells/μL, platelet count of 70.0 × 10^4 cells/μL, hemoglobin level of 10.2 g/dL, and hematocrit value of 33.4%. Additionally, the BUN and Cre concentrations were within the reference range, at 12.6 mg/dL and 0.83 mg/dL, respectively.

Abdominal ultrasonography utilizing a 7.5-MHz linear probe (APLIO ARTIDA SSH-880CV; CANON Medical Systems Co., Ltd., Ootawara, Japan) confirmed a single large mass measuring approximately 26 × 20 cm in size, located in the right abdominal cavity containing moderately echogenic fluid (Fig. 1A) and some fibrin-like material at the border of the normally appearing tissue of the right kidney (Fig. 1B).

Computed tomography (CT) was performed to obtain detailed information about the mass. Xylazine hydrochloride at a concentration of 2% (0.2 mg/kg, Selactar; Elanco Japan K.K., Tokyo, Japan) was intravenously administered to sedate the calf, and CT was performed using a helical 16-row multi-detector CT system (Aquilion Lightning TSX-035A; Canon Medical Systems Inc.). The CT parameters were set as follows: tube voltage, 120 kV; tube current, 200 mA; tube rotation time, 0.5 sec/rotation; and slice thickness, 1.0 mm. Digital Imaging and Communications in Medicine data were sent to a viewer (Newton OsiriX; Newton-Graphics, Sapporo, Japan) to measure the CT number and length of the lesion.

A portion of the right kidney and a contiguous cystic structure were observed on the plain CT image (Fig. 2A). Contrast-enhanced CT was then performed, using Iohexol (Iodine concentration 300 mgI/mL, Omnipaque 300; Daiichi Sankyo, Tokyo, Japan). The contrast agent was administered intravenously to the patient at a rate of 2 mL/kg body weight, and images were taken immediately after administration and at 3 and 7 min later. After 7 min, a normal portion of the right kidney was contrasted, and no migration of contrast media was visible in the large (24.1 × 20.2 cm) mass, which was visible in both the transverse (Fig. 2B) and sagittal planes (Fig. 2C). The CT value of the mass content was 10–13 HU, suggesting fluid retention. Additionally, the contrast media was visible in the right and left ureters extending from the kidney to the bladder, without signs of obstruction.

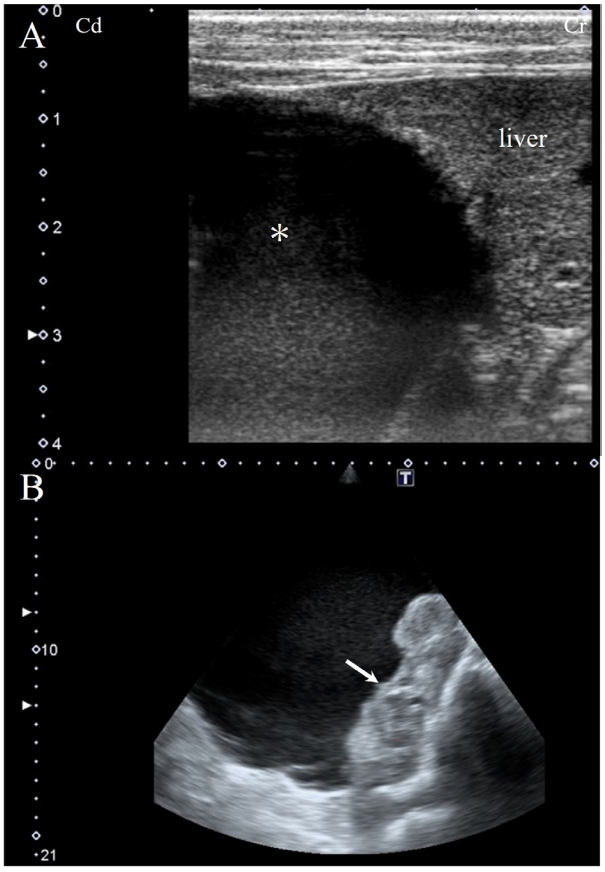

Fig. 1. Transabdominal ultrasound image from the right flank with a 7.5-MHz liner probe. A large mass filled with fluid extending from the right flank to the liver (asterisk; A) and fibrin-like material in the mass are visible (arrow; B).

Based on the results of ultrasound and CT imaging, the patient was suspected to have developed hydronephrosis of half of the right kidney due to urine outflow obstruction.

Based on the age in months, we suspected congenital disease. In addition, an investigation of the mother, siblings, and half-siblings conceived using the same semen sample and unrelated cattle housed in the same ranch was performed. None of them had previously developed similar diseases. The calf was also tested for kidney-related IARS deficiency, Claudin-16 deficiency, Molybdopterin cofactor sulfurase deficiency, and Bartter syndrome type 1 genes, all of which showed negative results.

As the calf was in good general condition and blood test results were normal, a right nephrectomy was performed. The calf was fasted for 12 hr before surgery. Cefazolin sodium (5 mg/kg) and flunixin meglumine (2 mg/kg; Forvet50; MSD, Tokyo, Japan) were administered intravenously to prevent perioperative infection and for pain relief, respectively. Subsequently, the calf was sedated with an intravenous injection of xylazine hydrochloride (0.2 mg/kg) and positioned in the left lateral recumbency. Isoflurane (Isoflu; Zoetis Japan, Tokyo, Japan) was administered continuously at a concentration of 2% in oxygen to induce and maintain general anesthesia. For local anesthesia, procaine hydrochloride (Adsan; Riken Vets Pharma, Iruma, Japan) was injected subcutaneously around the incision line at the right paralumbar fossa.

A vertical skin incision of 20 cm in length was performed in the right paralumbar fossa at 2 cm caudal to the last rib, starting dorsally at 2 cm ventral to the lumbar transverse processes. The muscle layers and the peritoneum were then incised to open the abdomen, exposing the enlarged right kidney. The retroperitoneal area was accessed by dissecting the surrounding tissue (peritoneum and fat) with a vessel sealing device (LigaSureTM Smart Jaw; Medtronic plc, Dublin, Ireland). The trajectories of the posterior vena cava and the abdominal aorta were confirmed, and the right renal artery, renal vein, and ureter were dissected from the surrounding fatty tissue.

The renal artery and vein were each ligated approximately 1 cm apart, and the vessels transected in between. The right kidney was pulled out of the abdominal cavity through the incision. The ureter was ligated approximately 1 cm apart close to the attachment to the bladder and transected in between, followed by kidney removal. The renal artery, renal vein, and ureter were ligated using synthetic, absorbable, multifilament polyglycolic acid suture material (USP 3+4, Opepolyx; Alfresa Pharma, Osaka, Japan). The peritoneum and muscular layer were closed using Opepolyx (USP 3+4) in a continuous suture pattern. The subcutaneous tissue was closed with

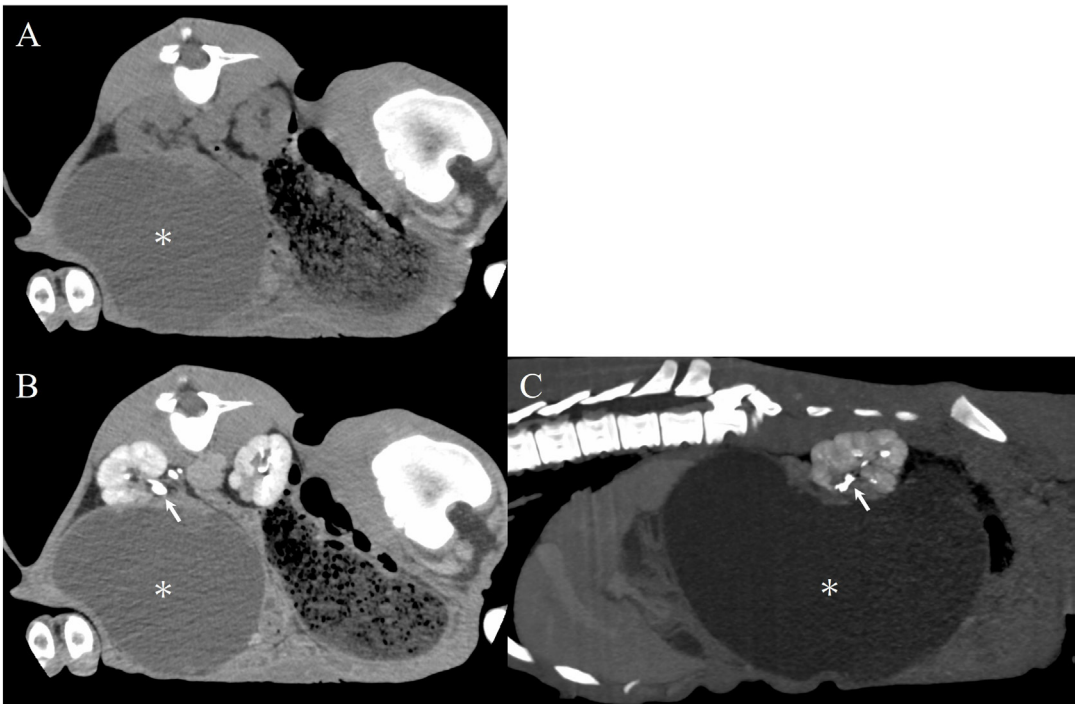

Fig. 2. On plain CT images in the transverse plane, a large mass (asterisk) with a cystic structure adjacent to the right kidney is observed (**A**). Contrast-enhanced CT image of the transverse plane (**B**) and sagittal plane (**C**). After contrast agent injection, the intrarenal ureters were depicted; the contrast agent did not enter the cyst, indicative of ureteral obstruction. The arrow indicates the intra-renal ureter. CT, computed tomography.

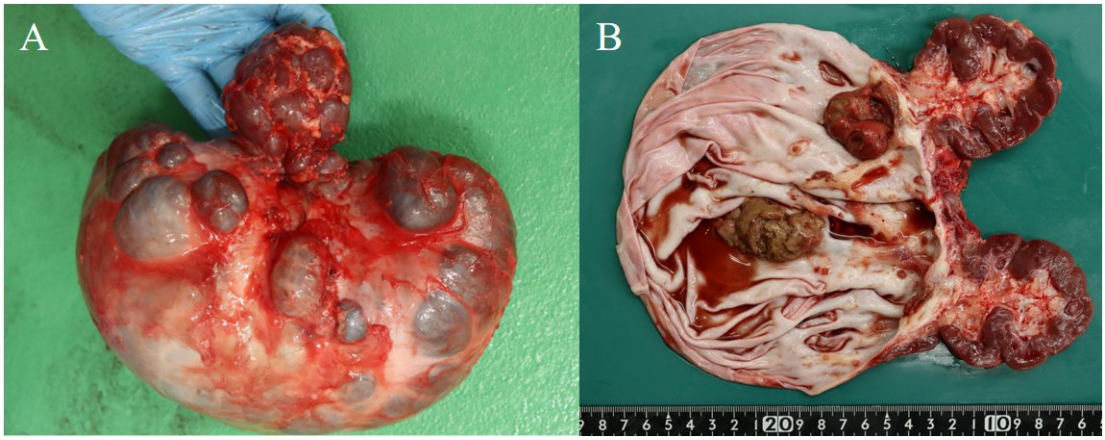

Fig. 3. The resected right kidney measured 24 × 20 × 10 cm and weighed 2.8 kg (**A**). Approximately half of the kidney had a gross normal structure, and the other half was greatly enlarged containing 2.3 L of dark reddish-purple fluid (**B**). Illustration of a cut surface of the removed kidney. The white arrow indicates fibrinonecrotic material in the kidney (**C**).

continuous sutures using polyglactin 910, a synthetic absorbable multifilament suture material (USP 0, Vicryl, Johnson & Johnson, Tokyo, Japan). The skin incision was closed with intradermal buried sutures using the same suture thread used for the subcutaneous tissue. Postoperatively, a compound drug containing 200,000 units of benzylpenicillin procaine and 250 mg of dihydrostreptomycin sulfate (0.05 mL/kg, Mycillin Sol; Meiji-Seika Pharma, Tokyo, Japan) was administered intramuscularly for 3 days. The calf recovered well from the surgical intervention and was discharged on postoperative day 3. At 28 months of age, which was more than 2 years after surgery, the animal was slaughtered along with a cow of similar age from the same farm.

Grossly, the resected right kidney measured 24 × 20 × 10 cm and weighed 2.8 kg (Fig. 3A). Approximately half of the kidney appeared normal macroscopically. The other half was markedly enlarged, with a massive fluid-filled cystic dilatation containing 2.3 L of a dark reddish-purple fluid (Fig. 3B). The intrarenal ureter of the right kidney was extremely narrow at the transition from the normal to the affected part.

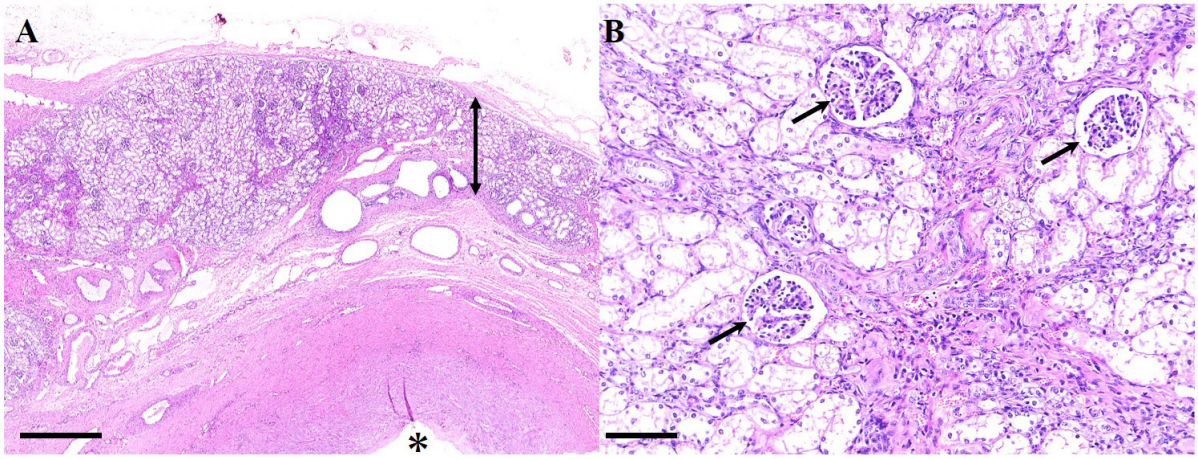

Fig. 4. Hydronephrosis in a Japanese black calf. (**A**) Atrophied renal parenchyma (double head arrow) and a dilated renal calyx (asterisk). Hematoxylin and eosin (H&E) stain (bar; 2.5 mm). (**B**) At high magnification, atrophied renal parenchyma showed renal glomeruli (arrows) and degenerated renal tubules with interstitial fibrosis. Hematoxylin and eosin stain (bar; 250 µm).

Histological and bacteriological examinations using tissues obtained by renal biopsy under ultrasound examination may be useful to characterize renal disease in bovines [20]. Histological analysis of the excised kidney revealed severe atrophy in the renal parenchyma with dilated renal calyces. The renal cortex showed renal glomeruli and degenerated renal tubules with interstitial fibrosis; degenerated renal tubules and dilated lymphatic vessels were observed in the renal medulla, while the renal calyx was markedly dilated (Fig. 4). These findings support the diagnosis of hydronephrosis of half of the right kidney. Additionally, a large amount of necrotic debris composed of necrotic transitional epithelium and fibrin exudate, with neutrophil and plasma cell infiltration, was found within the cystic lesion. There was no undifferentiated mesenchyme in the right kidney. Furthermore, the remaining half of the right kidney did not show any cystic lesions. Bacterial growth was not detected in the preoperative urine sample cultures or fluid from the resected kidney.

The postoperative blood chemistry findings revealed that the BUN and Cre levels increased immediately after surgery, peaking on postoperative day 3 and then gradually decreasing until they reached preoperative levels on postoperative day 10 (Fig. 5). While BUN and Cre are commonly utilized to assess renal function through blood tests, they possess limited sensitivity in detecting minor renal damage and typically do not deviate from reference values unless the condition has significantly deteriorated [17, 28]. This is because in unilateral kidney disease or incomplete urinary retention, the unaffected kidney can compensate for the damaged one.

In the present case, the left kidney was morphologically normal, and the right kidney maintained a partially normal morphology. The preoperative BUN and Cre levels were within the normal range, presumably because the renal injury was not severe. Following nephrectomy, the remaining kidney was temporarily overloaded, and BUN and Cre concentrations peaked on postoperative day 3 before decreasing to normal values, due to compensatory function. The concentrations reverted to preoperative levels on day 10 after nephrectomy, indicating that immediate postoperative blood tests may not be suitable for assessing residual renal function after nephrectomy.

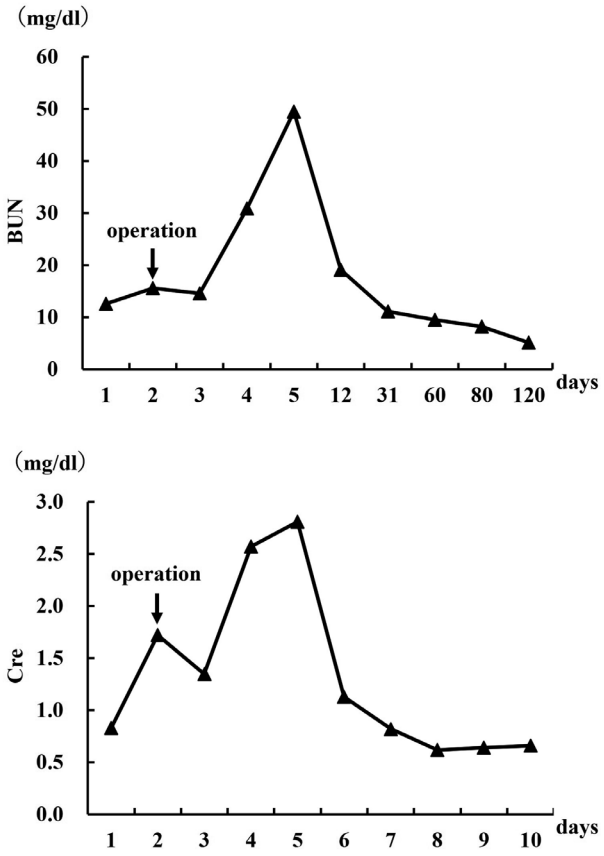

Fig. 5. Line diagram representing perioperative levels of blood urea nitrogen (BUN) and blood creatinine (Cre). operation=nephrectomy.

Hydronephrosis is a dilatation of the renal pelvis and calyces associated with progressive atrophy and cystic enlargement of the kidney [18]. In our case, half of the right kidney was significantly enlarged as a massive fluid-filled cystic dilatation. Microscopically,

this half revealed severe atrophy in the renal parenchyma, with markedly dilated renal calyces. Macroscopic and microscopic findings in our case support the diagnosis of hydronephrosis. Hydronephrosis has been previously described in a calf, where half of the kidney was hydronephrotic, as a massive fluid-filled cystic dilatation. Microscopically, it showed severe atrophy of the cortex and medulla [2], similar to what was observed in the present case. Hydronephrosis should be differentiated from other cystic renal diseases including multicystic renal dysplasia, polycystic kidney disease (PKD), and simple renal cysts (SRCs), which should be considered in the differential diagnosis [18]. Multicystic renal dysplasia is a variant of renal dysplasia in which a dysplastic kidney shows typical features of dysplasia with large cysts [27, 29]. PKD is characterized by numerous fluid-filled small cysts throughout the cortex and medulla, making it difficult to distinguish between the cortex and medulla both grossly and microscopically [18, 21, 25]. SRCs, which are usually incidental findings, arise from the surface of the kidney and may compress the adjacent cortex [9, 18]. SRCs are lined with a single cuboidal or flattened epithelial layer, and atrophic epithelial layers also can be occasionally observed [9]. In the present case, the hydronephrotic half of the right kidney did not show undifferentiated mesenchyme. In addition, neither undifferentiated mesenchyme nor cystic lesions were identified in the remaining half of the right kidney. These findings exclude the diagnoses of multicystic renal dysplasia or PKD. Based on these findings, polycystic renal dysplasia and PKD were excluded, and hydronephrosis was diagnosed instead.

The prognosis of hydronephrosis depends on whether it is bilateral, on the completeness of the obstruction, and on other complications of the obstruction, with unilateral cases being an indication for surgical intervention [18]. In humans, congenital hydronephrosis is generally bilateral, and therefore, surgical treatment is not considered [6, 15, 24]. In this case, the contralateral kidney was morphologically normal and had no potentially fatal hematologic burden; therefore, nephrectomy was performed, and the patient had a good outcome. BUN and Cre concentrations were temporarily elevated postoperatively but recovered to baseline levels by day 10.

In bovine hydronephrosis, nephrectomy may provide a favorable prognosis if one kidney is intact. Moreover, this case suggests that blood tests immediately after surgery are not suitable for evaluating residual kidneys.

CONFLICT OF INTEREST. The authors declare no conflict of interest.

ACKNOWLEDGMENTS. The authors thank the Livestock Improvement Association of Japan for the genetic examination, and the staff and student assistants at the University of Miyazaki for the care provided to the calves during hospitalization.

REFERENCES

1. Aldridge BM, Garry FB. 1992. Chronic partial obstructive urolithiasis causing hydronephrosis and chronic renal failure in a steer. *Cornell Vet* **82**: 311–317. [Medline]
2. Bazargani T, Khodakaram-Tafti A, Ashrafi I, Abbassi AM. 2015. Giant hydronephrosis and secondary pyelonephritis induced by Salmonella dublin in a Holstein calf. *Majallah-i Tahqiqat-i Dampizishki-i Iran* **16**: 114–116. [Medline]
3. Christoph F, Weikert S, Müller M, Miller K, Schrader M. 2005. How septic is urosepsis? Clinical course of infected hydronephrosis and therapeutic strategies. *World J Urol* **23**: 243–247. [Medline] [CrossRef]
4. Dare G, Akhtar M, Chaudhary S. 2019. Unilateral hydronephrosis in adults: etiology, clinical presentations and management. *Int Surg J* **6**: 2028–2031. [CrossRef]
5. Divers TJ. 2008. Urinary tract diseases. pp. 447–466. In: Rebhun's Disease of Dairy Cattle, 2nd ed. (Peek SF, Divers TJ eds.), Saunders Elsevier, Philadelphia.
6. Eskild-Jensen A, Gordon I, Piepsz A, Frøkiaer J. 2005. Congenital unilateral hydronephrosis: a review of the impact of diuretic renography on clinical treatment. *J Urol* **173**: 1471–1476. [Medline] [CrossRef]
7. Floeck M. 2007. Sonographic application in the diagnosis of pyelonephritis in cattle. *Vet Radiol Ultrasound* **48**: 74–77. [Medline] [CrossRef]
8. Fufezan O, Asavoaie C, Blag C, Popa G. 2011. The role of ultrasonography for diagnosis the renal masses in children. Pictorial essay. *Med Ultrason* **13**: 59–71. [Medline]
9. Gómez BI, Little JS, Leon AJ, Stewart IJ, Burmeister DM. 2020. A 30% incidence of renal cysts with varying sizes and densities in biomedical research swine is not associated with renal dysfunction. *Animal Model Exp Med* **3**: 273–281. [Medline] [CrossRef]
10. Harrison GD, Biller DS, Wilson DG, Castleman WL. 1992. Ultrasonographic diagnosis of hydronephrosis in a cow. *Vet Radiol Ultrasound* **33**: 49–51. [CrossRef]
11. Hayashi H, Biller DS, Rings DM, Miyabayashi T. 1994. Ultrasonographic diagnosis of pyelonephritis in a cow. *J Am Vet Med Assoc* **205**: 736–738. [Medline] [CrossRef]
12. Hirsbrunner G, Lang J, Nicolet J, Steiner A. 1996. Nephrectomy for chronic, unilateral suppurative pyleonephritis in cattle. *Tierarztl Prax* **24**: 17–21. [Medline]
13. Johnston JH, Evans JP, Glassberg KI, Shapiro SR. 1977. Pelvic hydronephrosis in children: a review of 219 personal cases. *J Urol* **117**: 97–101. [Medline] [CrossRef]
14. Juan HC, Tsia YF, Liu CC, Pan SC, Chang P, Huang CH, Huang SP. 2010. A giant bladder stone with bilateral hydronephrosis in a young male. *Urol Sci* **21**: 103–106. [CrossRef]
15. Legraverend JM, Ricard J, Boudailliez B, Le Van L, Kremp O, Baratte B, Canarelli JP. 1986. Treatment of hydronephrosis in newborn infants. Apropos of 18 cases diagnosed by antenatal ultrasonography. *J Urol (Paris)* **92**: 559–563. [Medline]
16. Lingard DA, Lawson TL. 1979. Accuracy of ultrasound in predicting the nature of renal masses. *J Urol* **122**: 724–727. [Medline] [CrossRef]
17. Macisaac RJ, Ekinci EI, Jerums G. 2014. Markers of and risk factors for the development and progression of diabetic kidney disease. *Am J Kidney Dis* **63** Suppl 2: S39–S62. [Medline] [CrossRef]
18. Maxie MG, Newmann SJ. 2007. The urinary system. pp. 425–522. In: Jubb, Kennydy & Palmers' Pathology of domestic animals, Vol. 2, 5th ed. (Maxie MG ed.), Saunders Elsvier, Philadelphia.

19. McDill BW, Li SZ, Kovach PA, Ding L, Chen F. 2006. Congenital progressive hydronephrosis (cph) is caused by an S256L mutation in aquaporin-2 that affects its phosphorylation and apical membrane accumulation. *Proc Natl Acad Sci USA* **103**: 6952–6957. [Medline] [CrossRef]
20. Mohamed T, Oikawa S. 2008. Efficacy and safety of ultrasound-guided percutaneous biopsy of the right kidney in cattle. *J Vet Med Sci* **70**: 175–179. [Medline] [CrossRef]
21. Nikkhah A, Alimirzaei M. 2023. Pyelonephritis and polycystic kidneys in a male Holstein calf. *J Vet Physiol Pathol* **2**: 9–11. [CrossRef]
22. Paudel D, Adhikari D, Dhakal RD. 2021. Moderate hydronephrosis among acute ureteral calculus on ultrasonographic imaging in a tertiary care center in Nepal: a descriptive cross-sectional study. *JNMA J Nepal Med Assoc* **59**: 1252–1255. [Medline] [CrossRef]
23. Radostits OM, Gay C, Hinchcliff KW, Constable PD. 2007. Veterinary medicine. pp. 966–994. In: A textbook of the diseases of cattle, horses, sheep, pigs and goats, 10th ed. (Radostits OM, Gay C, Hinchcliff KW, Constable PD, eds.), Saunders Elsevier, Edinburgh.
24. Shah SA, Ranka P, Dodiya S, Jain R, Kadam G. 2004. Giant hydronephrosis: What is the ideal treatment? *Indian J Urol* **20**: 118–122. [CrossRef]
25. Sonawane G, Swarnkar C. 2018. Pathology of congenital polycystic kidney disease in a stillborn foetus of fat-tailed (Dumba) sheep. *Indian J Small Ruminants* **24**: 101–105. [CrossRef]
26. Tyler JW, Smith BP, Irvine J. 1991. Hydronephrosis and pyelonephritis associated with an anomalous vas deferens in a bull. *J Am Vet Med Assoc* **198**: 871–872. [Medline]
27. Ushigaki K, Uchida K, Murakami T, Yamaguchi R, Tateyama S. 1999. Multicystic renal dysplasia in a Japanese black bull. *J Vet Med Sci* **61**: 839–842. [Medline] [CrossRef]
28. Vaidya VS, Bonventre JV. 2006. Mechanistic biomarkers for cytotoxic acute kidney injury. *Expert Opin Drug Metab Toxicol* **2**: 697–713. [Medline] [CrossRef]
29. Yoshida K, Takezawa S, Itoh M, Takahashi E, Inokuma H, Watanabe K, Kobayashi Y. 2022. Renal dysplasia with hydronephrosis and congenital ureteral stricture in two Holstein-Friesian calves. *J Comp Pathol* **193**: 20–24. [Medline] [CrossRef]